RIPK2 is crucial for the microglial inflammatory response to bacterial muramyl dipeptide but not to lipopolysaccharide

Changjun Yang[1], PhD; Maria Carolina Machado da Silva[1,2], MS; John A. Howell[1], PhD; Jonathan Larochelle[1], PhD; Lei Liu[1], PhD; Rachel E. Gunraj[1], BA; Antônio Carlos Pinheiro de Oliveira[1,2], PhD; Eduardo Candelario-Jalil[1*],PhD

[1]*Department of Neuroscience, McKnight Brain Institute, University of Florida, Gainesville, FL, USA*

[2]*Neuropharmacology Laboratory, Department of Pharmacology, Universidade Federal de Minas Gerais, Brazil*

***Corresponding author:** Eduardo Candelario-Jalil, Ph.D.

Department of Neuroscience, University of Florida, McKnight Brain Institute, 1149 SW Newell Drive, Gainesville, FL 32610, USA. Phone: (352)-273-7116. Fax: (352)-392-8347.

E-mail: ecandelario@ufl.edu

Running Title: Role of RIPK2 in microglial inflammatory responses

Abstract

Receptor-interacting serine/threonine protein kinase 2 (RIPK2) is a kinase that plays an essential role in the modulation of innate and adaptive immune responses. As a downstream signaling molecule for nucleotide-binding oligomerization domain 1 (NOD1), NOD2, and Toll-like receptors (TLRs), it is implicated in the signaling triggered by recognition of microbe-associated molecular patterns by NOD1/2 and TLRs. Upon activation of these innate immune receptors, RIPK2 mediates the release of pro-inflammatory factors by activating mitogen-activated protein kinases (MAPKs) and nuclear factor-kappa B (NF-κB). However, whether RIPK2 is essential for downstream inflammatory signaling following the activation of NOD1/2, TLRs, or both remains controversial. In this study, we examined the role of RIPK2 in NOD2- and TLR4-dependent signaling cascades following stimulation of microglial cells with bacterial muramyl dipeptide (MDP), a NOD2 agonist, or lipopolysaccharide (LPS), a TLR4 agonist. We utilized a highly specific proteolysis targeting chimera (PROTAC) molecule, GSK3728857A, and found dramatic degradation of RIPK2 in a concentration- and time-dependent manner. Importantly, the PROTAC completely abolished MDP-induced increases in iNOS and COX-2 protein levels and pro-inflammatory gene transcription of *Nos2*, *Ptgs2*, *Il-1β*, *Tnfα*, *Il6*, *Ccl2*, and *Mmp9*. However, increases in iNOS and COX-2 proteins and pro-inflammatory gene transcription induced by the TLR4 agonist, LPS, were only slightly attenuated with the GSK3728857A pretreatment. Further findings revealed that the RIPK2 PROTAC completely blocked the phosphorylation and activation of p65 NF-κB and p38 MAPK induced by MDP, but it had no effects on the phosphorylation of these two mediators triggered by LPS. Collectively, our findings strongly suggest that RIPK2 plays an essential role in the inflammatory responses of microglia to bacterial MDP but not to LPS.

Keywords

inflammatory response; microglia; muramyl dipeptide; lipopolysaccharide; receptor-interacting serine/threonine protein kinase 2; Toll-like receptor; nucleotide-binding oligomerization domain-like receptor; mitogen-activated protein kinase; nuclear factor-kappa B

1. Introduction

As two major forms of innate immune sensors, Toll-like receptors (TLRs) and nucleotide-binding oligomerization domain (NOD)-like receptors (NLRs) play an important role in the regocnition of pathogen-associated molecular patterns (PAMPs) to activate innate immunity and inflammatory responses against pathogenic invasion or tissue injury [1]. TLRs are transmembrane receptors that mediate bacterial recognition at the cell surface or in endosomes, where TLR4 is the most efficient member of the pattern recognition receptors (PRRs) recognized and activated by a wide variety of ligands [2]. In contrast, NLRs mediate innate immune responses through cytosolic recognition of bacterial components. NOD1 and NOD2 are two major NLRs, and they normally sense bacterial molecules produced during the synthesis and/or degradation of peptidoglycan (PGN) [3, 4].

NOD1 is activated upon binding to bacterial PGN fragments containing diaminopimelic acid (DAP) [3], whereas NOD2 recognizes muramyl dipeptide (MDP) constituents [4]. Recognition of PAMPs by NOD1 and NOD2 receptors leads to the interaction between the receptor-interacting serine/threonine protein kinase 2 (RIPK2, also known as RIP2, RICK, CARDIAK, and CARD3) and these innate immune receptors through caspase recruitment domain (CARD)-CARD interaction. This is followed by the release of pro-inflammatory factors through the activation of mitogen-activated protein kinases (MAPKs), thereby leading to

stimulation of transcription factor activator protein-1 (AP-1) and/or nuclear factor-kappa B (NF-κB) [5, 6]. As a critical mediator modulating the pro-inflammatory signaling pathway, pharmacological inhibition, genetic deletion, or degradation using the proteolysis targeting chimera (PROTAC) of RIPK2 might be beneficial in reducing inflammation in diseases such as ischemic stroke, inflammatory bowel disease, and rheumatoid arthritis.

While several reports show that RIPK2 is critical for inflammatory signaling in peripheral immune cells, little is known about the role of RIPK2 in microglia, the main tissue-resident macrophage of the CNS. Several neurological diseases are known to be associated with microglia-driven inflammation, in which NOD2 and/or TLR4/myeloid differentiation primary response protein 88 (MyD88) signaling pathways are actively involved. For example, emerging evidence indicates that ischemic stroke induces gut permeability and enhances bacterial translocation to the ischemic brain and periphery, thus resulting in a rapid response of peripheral immune cells and activation of astroglial/microglial cells to release more pro-inflammatory factors, which could exacerbate ischemic brain injury [7-10]. In agreement with this notion, RIPK2 was found to be upregulated in a time-dependent manner during brain ischemia/reperfusion injury. Mice deficient in RIPK2 exhibited reduced inflammatory response and neuronal apoptosis, with smaller infarct volume and improved neurological deficits score, while neuron-specific RIPK2 overexpressing transgenic mice displayed worse stroke outcomes compared with the wild-type (WT) controls [11].

Our recent findings also demonstrated that mice with global genetic deletion of RIPK2 or conditional deletion of microglial RIPK2 showed reduced effects on infarct volume and improved neurobehavioral outcomes after ischemic stroke compared to their WT littermates [12]. Also, NOD1 and RIPK2 were found to be increased in response to intracerebral

hemorrhage (ICH) and contributed to microglial activation and the inflammatory response, while either inhibition of NOD1 with ML130 (a highly selective inhibitor of NOD1) or RIPK2 with GSK583 (a specific RIPK2 inhibitor) alleviated the ICH-induced brain damage, microglial activation, and inflammatory response in mice [13]. Treatment with a RIPK2 inhibitor at the onset of reperfusion after MCAO attenuated the RIPK2 phosphorylation induced by stroke and significantly reduced infarct volume and blood-brain barrier (BBB) disruption [14]. These findings indicate that RIPK2 is upregulated or activated in the ischemic brain and plays a detrimental role in the progression of stroke injury by increasing the neuroinflammatory response and microglial activation to stroke.

However, it still remains controversial whether the receptors of NOD1/2, TLRs or both mediate RIPK2 signaling pathways [5, 6, 15-18], thus resulting in inflammatory responses in pathophysiological conditions. In the present study, we have examined the role of RIPK2 in NOD2- and TLR4-dependent signaling cascades under the stimulation of MDP (a NOD2 agonist) or lipopolysaccharide (LPS, a TLR4 agonist) in microglial cells. Our findings strongly suggest that RIPK2 plays an essential role in the inflammatory responses of microglia to the stimulation by bacterial MDP but not to LPS.

2. Materials and methods

2.1. Cell culture

The SIM-A9 mouse microglial cell line was grown in a T75 flask with complete growth media composed of 84% DMEM/F12 media (Cat. No. SH30023.01; HyClone, Cytiva, Marlborough, MA), 10% heat-inactivated fetal bovine serum (Cat. No. F4135, MilliporeSigma), 5% heat-inactivated horse serum (Cat. No. 16050130, ThermoFisher Scientific, Waltham, MA),

and 1% of penicillin-streptomycin (Cat. No. 15140122; ThermoFisher Scientific) and maintained at 37 °C in a 5% CO_2 incubator [19, 20]. The cells were subcultured every 2-3 days.

2.2. Treatments and harvest of microglial cells

For assigned experiments, cells were seeded at a density of 3.6×10^4 cells/cm^2 in a 60-mm dish pre-coated with 50 µg/mL of poly-D-lysine (Cat. No. P6407, MilliporeSigma, St. Louis, MO) with 4 mL of complete growth media and maintained at 37°C under 5% CO_2. After growing overnight, cells were incubated for 4 hours with different concentrations (0-10 µM) of RIPK2 proteolysis targeting chimera (PROTAC) GSK3728857A (hereafter referred to as RIPK2 PROTAC, obtained from GlaxoSmithKline under material transfer agreement number UK-JH-MTA3000037627) [21] for the dose-response experiment or varying incubation periods (0-24 h) with 1 µM of RIPK2 PROTAC for the time-course study. For optimizing the concentration of NOD2 agonist used in the following studies, cells were exposed to various concentrations (0 to 10 µg/mL) of muramyl dipeptide (MDP, a bacterial cell wall component) (Cat. No. tlrl-lmdp, InvivoGen, San Diego, CA) for 24h. After confirming the optimal concentration of MDP, cells were treated with 100 ng/mL MDP with different incubation times to determine phosphorylated protein levels involved in NF-κB and p38 MAPK signaling pathways. Also, cells were pretreated with either DMSO or the optimized concentration of RIPK2 PROTAC (1 µM) for 4h followed by 20h incubation of 100 ng/mL MDP or 10 ng/mL lipopolysaccharide (LPS) (Cat. No. L9641, MilliporeSigma). At the end of each incubation time, media were harvested for cell viability analysis, and cells were rinsed with ice-cold phosphate-buffered saline (PBS) and collected with 200 µL of radioimmunoprecipitation (RIPA) lysis buffer consisting of 50 mM Tris-HCl (pH 7.4), 150 mM NaCl, 5 mM EDTA, 1 mM EGTA, 1% NP-40, 0.5% sodium deoxycholate and 0.1% SDS plus protease and phosphatase inhibitor cocktails (Cat. Nos. 78430 and 78428,

respectively; ThermoFisher Scientific). Half of the cell lysate volume was used for RNA isolation, and the other half was used for protein extraction, as described previously [20].

2.3. Immunoblotting analysis

Thirty micrograms of protein were denatured in 2× Laemmli sample buffer (Cat. No. 1610737, Bio-Rad, Hercules, CA) containing 4% β-mercaptoethanol at 100 °C for 5 min before loading into 4-20% SDS-polyacrylamide gels. After gel running, they were transferred onto nitrocellulose membranes and then blocked for 1 h at room temperature with Intercept (TBS) Blocking Buffer (Cat. No. 927-60001, LI-COR Biotechnology, Lincoln, NE). After that, the membranes were incubated at 4°C overnight with primary antibodies rabbit anti-RIPK2 (1:1000; Cat. No. 4142; Cell Signaling Technology, Danvers, MA), rabbit anti-iNOS (1:1000; Cat. No. ab15323; Abcam, Cambridge, MA), rabbit anti-COX-2 (1:2000; Cat. No. ab15191; Abcam), rabbit anti-phospho-NF-κB p65 (1:1000; Cat. No. 3033; Cell Signaling Technology), rabbit anti-phospho-p38 MAPK (1:1000; Cat. No. 4631; Cell Signaling Technology), or rat anti-β-actin antibody (1:5000; Cat. No. 664801; BioLegend, San Diego, CA) in Intercept T20 (TBS) Antibody Diluent (CAT#: 927-65001). The membranes were then washed with TBST three times at 5 min intervals, incubated with goat anti-rabbit IRDye 800CW (1:30000; Li-Cor, Lincoln, NE) or goat anti-rat IRDye 680LT (1:40000; Li-Cor) secondary antibodies for 1h at room temperature. Immunoreactive bands were visualized and densitometrically analyzed using Odyssey infrared scanner and Image Studio 2.0 software (Li-Cor).

2.4. RNA extraction

The remaining half of the cell lysate was mixed with 1.0 mL of TRIzol solution (Cat. No. 15596026; ThermoFisher Scientific) to be processed for RNA isolation. Briefly, 200 µL of chloroform was added to the mixture of cell lysates/TRIzol and vortexed well, incubated at

room temperature for 3 min, then centrifuged at 12,000 ×g for 15 min at 4 °C. The upper aqueous phase was saved and mixed with an equal volume of 70% ethanol, vortexed thoroughly before filtering the mixture on a silica column (Cat. No. SD5008; Bio Basic) at 12,000 ×g for 1 min at 4°C. After filtration, the nucleic acids bound to the silica resin of the column were washed with 250 µL of washing buffer A (1.0 M Guanidine thiocyanate, 10 mM Tris, pH 7.0) and spun down at 12,000 ×g for 1 min. For DNA removal, 75 µL of DNase I digestion mixture (66 µL nuclease-free water + 1.5 µL DNase I (Cat. No. 6344; Worthington Biochemical Corporation, Lakewood, NJ) + 7.5 µL of 10X NEB DNase I Reaction Buffer (Cat. No. B0303S; New England BioLabs® Inc., Ipswich, MA) was added to the silica resin bed of the column, and incubated at room temperature for 15 min. The column was washed again by adding 250 µL of washing buffer A and spun down at 12,000 ×g for 1 min. The filtrate was discarded, and the silica column bound with RNA sample was washed with 500 µL of washing buffer B (10 mM Tris, pH 7.0 in 80% ethanol) and spun down at 12,000 ×g for 1 min. After that, the RNA sample was washed with the washing buffer B again and spun down a final time at 16,000 ×g for 2 min. Then the silica column was transferred to a new 1.5 mL nuclease-free microcentrifuge tube, and 50 µL of nuclease-free water (pre-warmed at 70 °C) was added to the center of the column, incubated at room temperature for 3 min. The RNA was eluted by spinning at 16,000 ×g for 2 min. The RNA concentration and purity were measured by absorbance (260/280 ratio) using a Take3 Micro-Volume Plate Reader (Biotek Instruments, Winooski, VT).

2.5. Real-time qPCR

Real-time quantitative PCR reactions were conducted in a 96-well plate using a CFX96 Touch Real-Time PCR System (Bio-Rad). Each reaction was performed in a 10 µL volume

containing 1× Luna Universal One-Step Reaction Mix plus 1× Luna WarmStart® RT Enzyme Mix (Cat. No. E3005; New England BioLabs® Inc.), 0.4 µM of each primer and 2 µL of 10 ng/µL RNA, using the following thermal conditions: 55 °C for 10 min, 95 °C for 1 min, followed by 40 cycles of 95°C for 10 seconds and 60 °C for 30 seconds. A melting curve analysis (60 °C to 95 °C) was performed at the end of each PCR to further confirm the amplicons' specificity. Primer sequences for *Nos2, Ptgs2, Il-1β, Tnfα*, *Il6*, *Ccl2*, *Mmp9*, and housekeeping genes *Cyc1* and *Rltr2aiap* were included in **Table 1**. Each sample was run in duplicate, and cycle threshold (Ct) values were normalized to the housekeeping genes *Cyc1* and *Rltr2aiap* (one of the expressed repetitive elements) since they are universally stable and widely used as reference genes under various conditions [22, 23].

Table 1. Primer sequences used for real-time PCR

Gene	Accession Number	Forward	Reverse
Nos2	NM_010927	5'-GTTCTCAGCCCAACAATACAAGA-3'	5'-GTGGACGGGTCGATGTCAC-3'
Ptgs2	NM_011198	5'-CAAGACAGATCATAAGCGAGGA-3'	5'-GCGCAGTTTATGTTGTCTGTC-3'
Il-1β	NM_008361	5'-GACCTGTTCTTTGAAGTTGACG-3'	5'-CTCTTGTTGATGTGCTGCTG -3'
Tnfα	NM_013693	5'-AGACCCTCACACTCAGATCA-3'	5'-TCTTTGAGATCCATGCCGTTG-3'
Il-6	NM_031168	5'-AGCCAGAGTCCTTCAGAGA-3'	5'-TCCTTAGCCACTCCTTCTGT -3'
Ccl2	NM_011333	5'-CATCCACGTGTTGGCTCA-3'	5'-AACTACAGCTTCTTTGGGACA-3'
Mmp9	NM_013599	5'-GACATAGACGGCATCCAGTATC-3'	5'-GTGGGAGGTATAGTGGGACA-3'
Cyc1	NM_025567	5'-CCAAAACCATACCCTAACCCT-3'	5'-CTGCTCACTGGCTACTGTG-3'
Rltr2aiap	N/A	5'-CATGTGCCAAGGGTAGTTCTC-3'	5'-GCAAGAGAGAGAGAATGGCGAAAC-3'

2.6. Statistical analysis

Data were expressed as mean ± SEM from at least three independent experiments and were analyzed using GraphPad Prism version 8 (GraphPad Software, San Diego, CA) with a one-way ANOVA followed by Bonferroni post hoc test. A value of $P < 0.05$ was considered statistically significant.

3. Results

3.1. Degradation of RIPK2 by its proteolysis targeting chimera in a dose- and time-dependent manner

To determine whether endogenous RIPK2 is degraded by GSK3728857A, a RIPK2 proteolysis targeting chimera (PROTAC) (**Fig. 1A, B**), SIM-A9 mouse brain microglial cells were incubated for 4 hours with various concentrations of RIPK2 PROTAC (0-10 μM) and the protein levels of RIPK2 were measured by western blot. As observed, RIPK2 PROTAC dose-dependently reduced the RIPK2 levels in the microglial cells (**Fig. 1C, D**). Incubation with the optimized concentration of RIPK2 PROTAC (1 μM) for increasing amounts of time exhibited a time-dependent degradation of RIPK2 (**Fig. 1E, F**). These results indicate that the RIPK2 PROTAC produces a robust proteolytic degradation of RIPK2 in microglia.

3.2. Microglia depend on RIPK2 to mount an inflammatory response to MDP

It is well documented that RIPK2 is a CARD-containing serine/threonine kinase that physically associates with the CARD of NOD1 or NOD2 through CARD-CARD interactions. In peripheral macrophages, activation of the NOD2 by its specific ligand MDP results in the recruitment of RIPK2, which will trigger the production of proinflammatory mediators through NF-κB and MAPK signaling [24]. The role of RIPK2-dependent signaling to activate the

microglial inflammatory response to NOD2 or TLR4 ligands is unknown. We first investigated whether SIM-A9 microglia respond to MDP. As shown in **Fig. 2**, incubation of microglial cells with various concentrations of MDP (0 to 10000 ng/mL) for 24 hours dose-dependently increased pro-inflammatory gene expression of *Nos2*, *Il-1β*, *Tnfα*, *Il6* and *Mmp9*. Also, the cell viability assay did not reveal any cytotoxic effect of MDP at any concentration studied (data not shown). For further experiments, we used 100 ng/mL MDP as it was the lowest concentration to induce the maximum inflammatory responses attainable with MDP in the microglial cells.

To assess the contribution of RIPK2 to NOD2- and Toll-like receptor 4 (TLR4)-mediated inflammatory responses, microglial cells were pretreated with 1 μM RIPK2 PROTAC for 4 hours followed by 20 hours incubation with 100 ng/mL MDP, the NOD2 agonist, or 10 ng/mL LPS, the TLR4 agonist. Treatment with RIPK2 PROTAC completely abolished the MDP-induced gene expression of classical proinflammatory mediators, such as *Nos2*, *Ptgs2*, *Il-1β*, *Tnfα*, *Il6*, *Ccl2* and *Mmp9* (**Fig. 3A**) and iNOS protein level (**Fig. 3B, C**), which was associated with significant RIPK2 degradation (**Fig. 3B, E**). Of interest, RIPK2 PROTAC reduced the effects of MDP-induced *Ptgs2* mRNA expression (**Fig. 3A**), but it had no significant effects on COX-2 protein level (**Fig. 3B, D**). Similar to a previous report that MDP treatment induces rapid proteasomal degradation of NOD2 and RIPK2 in RAW264.7 macrophage cells [25], our findings indicated that MDP treatment dramatically reduced RIPK2 protein level in the microglia compared to unstimulated cells (**Fig. 3B, E**).

It is known that proinflammatory gene transcription induced by NOD1 and NOD2 is mediated through NF-κB transcription factor and MAPK signaling pathways [24]. To determine which downstream effector was involved in MDP/NOD2-mediated inflammatory responses in

microglia, phosphorylated protein levels of NF-κB p65 and p38 MAPK were measured in MDP-stimulated SIM-A9 cells with and without RIPK2 PROTAC pretreatment. As shown in **Fig. 4A**, MDP increased phosphorylation of NF-κB p65 and p38 MAPK, and 60 min incubation with MDP induced the maximal effects on both phosphorylated protein levels. Such activation of NF-κB p65 and p38 MAPK in response to MDP was abolished entirely in microglia in the presence of RIPK2 PROTAC (**Fig. 4B-D**). Taken together, these findings strongly suggest that RIPK2 is essentially involved in the MDP-mediated activation of NF-κB and p38 MAPK signaling pathways, which contribute to the proinflammatory response of microglia to MDP treatment.

3.3. RIPK2 is only partially required for LPS-mediated inflammatory response in microglia

Next, we examined the effects of RIPK2 PROTAC on LPS-stimulated immune inflammatory responses in the SIM-A9 cells since it remains controversial whether RIPK2 contributes to NOD1/2 signaling, TLR signaling, or both [5, 6, 15-18]. Compared with the effects of MDP on proinflammatory gene transcription, LPS has a more potent ability to stimulate inflammatory gene expression. As shown in **Fig. 5A-D**, quantitative RT-PCR and immunoblots indicate that proinflammatory genes, including *Nos2*, *Ptgs2*, *Il-1β*, *Tnfα*, *Il6*, *Ccl2,* and *Mmp9,* as well as protein levels of iNOS and COX-2 were dramatically upregulated by LPS in microglia. Degradation of RIPK2 by the RIPK2 PROTAC partly attenuated LPS-induced *Ptgs2*, *Il-1β*, *Il6*, *Ccl2* and *Mmp9* gene transcription and COX-2 protein, but it had no significant effects on the mRNA expression of *Nos2* and *Tnfα* or iNOS protein level induced by LPS. Unlike the effects mediated by MDP, increases in phosphorylation of NF-κB p65 and MAPK p38 by LPS were not attenuated with the pretreatment of the RIPK2 PROTAC (**Fig. 5B, E and**

F). Also, LPS alone robustly increased RIPK2 levels compared to the control cells (**Fig. 5B, G**), which is in agreement with previous reports that LPS can sustainedly increase RIPK2 levels in macrophages isolated from mice or in the RAW264.7 macrophage cell line [5, 25]. Collectively, these findings suggested that RIPK2 is not essential for microglia during an LPS/TLR4-mediated inflammatory response.

4. Discussion

In the current study, we have compared the role of RIPK2 in MDP/NOD2- and LPS/TLR4-mediated signaling pathways that essentially contribute to inflammatory responses in microglial cells. We found that PROTAC-mediated degradation of RIPK2 is concentration- and time-dependent in SIM-A9 microglia. Incubating SIM-A9 cells with MDP, the agonist of NOD2, increased pro-inflammatory gene expression of *Nos2, Il-1β, Tnfα, Il6,* and *Mmp9* in a concentration-dependent manner. Depletion of RIPK2 with the PROTAC molecule completely abolished the effects of MDP-induced iNOS and COX-2 protein levels and pro-inflammatory gene transcription of *Nos2, Ptgs2, Il-1β, Tnfα, Il6, Ccl2* and *Mmp9*. However, increases of iNOS and COX-2 proteins, as well as seven pro-inflammatory genes induced by TLR4 agonist, LPS, were slightly attenuated with the pretreatment of the RIPK2 PROTAC. Further findings revealed that the RIPK2 PROTAC completely blocked the activation of p65 NF-κB and p38 MAPK induced by MDP, but it had no effects on the phosphorylation of these two mediators triggered by LPS. Taken together, our findings strongly suggest that RIPK2 plays a crucial role in the inflammatory responses of microglia to bacterial MDP but not LPS.

A considerable number of studies have demonstrated that RIPK2 acts as an adaptor in immune response and inflammation process, transducing signals either from NODs (NOD1

and NOD2) or TLRs, thus leading to the activation of MAPKs and NF-κB, followed by the subsequent production of proinflammatory factors [5, 6, 15-18]. Several studies using RIPK2 deficient mice suggested that RIPK2 is involved in TLR signaling, such as LPS/TLR4 signaling, and the absence of RIPK2 conferred reduced inflammatory responses in macrophages stimulated by LPS [5, 16, 18]. In human monocyte-derived dendritic cells, knockdown of RIPK2 by siRNA blocked LPS-induced activation of p38 MAPK and NF-κB signaling, thus reducing the expression of IL-12, a critical factor for the generation of the Th1 type immune response [26]. In line with these observations, trinitrobenzene sulfonic acid (TNBS)- or dextran sodium sulfate (DSS)-induced colitis was ameliorated by administration of siRNA targeting RIPK2 in NOD2- or NOD1/NOD2-double deficient mice [17], indicating that the effect of RIPK2 depletion on colitis can occur independently of either NOD1 or NOD2 signaling and TLRs-dependent gut inflammation might be involved. In contrast to these reports, a study examined both innate and adaptive immune responses in RIPK2 deficient mice and no significant differences in IL-6 or TNFα production were observed in bone marrow-derived macrophages from RIPK2 knockout or WT mice when stimulated with LPS (TLR4 agonist), poly(I:C) (TLR3 agonist), CpG (TLR9 agonist), or Pam3Cys-SKKKK (Pam3; synthetic peptide specific for TLR2), while NOD1/2 signaling was impaired in macrophages from RIP2-deficient mice [15], indicating that RIPK2 is a downstream effector of NOD1/2- instead of TLRs-signaling that contributes to innate immune responses in macrophages. Consistent with this observation, Park *et al*. [6] demonstrated that macrophages and mice lacking RIPK2 were defective in their responses to NOD1 and NOD2 agonists but exhibited unimpaired responses to highly purified TLR ligands. Activation of NF-κB and MAPKs by LPS was greatly inhibited or abolished in TLR4-null macrophages but was unaffected in RIPK2 deficient macrophages. Such activation of NF-κB and MAPKs by MDP,

the NOD2 agonist, was abrogated in RIPK2 deficient macrophages. Furthermore, the absence of RIPK2 or double deficiency of NOD1 and NOD2 was associated with reduced IL-6 production in *Listeria*-infected macrophages. These results suggest that RIPK2 mediates innate immune response induced through NOD1 and NOD2, but not TLRs. To explore this conflicting observation of whether RIPK2 acts as a downstream mediator of NOD1/2, TLRs, or both, we conducted studies investigating MDP/NOD2- and LPS/TLR4-mediated proinflammatory pathways in primary microglial cells in which RIPK2 was profoundly depleted by proteolytic degradation with the RIPK2 PROTAC. Notably, PROTAC-mediated protein degradation has emerged as a novel therapeutic strategy to tackle disease-causing aberrant proteins since PROTACs exhibit unprecedented efficacy and specificity in degrading target proteins compared to traditional small molecule inhibitors. Here, we employed GSK3728857A [21], a potent and effective RIPK2 PROTAC, in specifically targeting RIPK2 degradation to test the contribution of RIPK2 in MDP/NOD2- and LPS/TLR4-mediated inflammatory pathway in primary microglial cells. Consistent with studies suggesting that RIPK2 acts as a downstream effector of NOD1/2 instead of TLRs signaling [6, 15], we found that deletion of RIPK2 with the PROTAC completely abolished the effects of MDP on activation of p65 NF-κB and p38 MAPK as well as the related proinflammatory gene transcription including *Nos2, Ptgs2, Il-1β, Tnfα, Il6, Ccl2* and *Mmp9*. The RIPK2 PROTAC slightly attenuated the inflammatory responses triggered by LPS, a TLR4 agonist. However, the PROTAC-mediated degradation of RIPK2 did not affect LPS-stimulated phosphorylation of p65 NF-κB and p38 MAPK, suggesting that a RIPK2-independent pathway might be involved in LPS/TLR4-induced proinflammatory responses in SIM-A9 microglial cells. However, our study cannot formally rule out the possibility that LPS stimulation may contribute directly or indirectly to NOD1/2-mediated

signaling. Of particular note, PGN molecules capable of stimulating NOD1 and NOD2 are commonly present in preparations of TLRs-stimulating components such as LPS preparation, and the presence of such contaminants could potentially explain the observed TLRs signaling defects in RIPK2 deficient macrophages [3, 27-29]. In agreement with this notion, Park *et al*. reported that deficiency of RIPK2 in macrophages or mice did not affect TLR signaling when highly purified TLR ligands were used for stimulations [6]. Taken together, our findings strongly suggest that RIPK2 plays an essential role in the inflammatory responses of microglia to bacterial MDP but not LPS, and further studies will be needed to explore the molecular basis for the cooperation between the receptors of NOD2 and TLR4. Our data could have important implications for understanding the complex interplay between NOD2- and TLR4-mediated inflammatory pathways in microglia, which is relevant for many neurological diseases associated with dysregulated microglial neuroinflammatory responses.

Author Contributions

Conceptualization, Changjun Yang and Eduardo Candelario-Jalil; Data curation, Changjun Yang and Eduardo Candelario-Jalil; Formal analysis, Changjun Yang, Antonio De Oliveira and Eduardo Candelario-Jalil; Funding acquisition, Eduardo Candelario-Jalil; Investigation, Changjun Yang, Maria Machado da Silva and Eduardo Candelario-Jalil; Methodology, Changjun Yang, Maria Machado da Silva, John Howell, Jonathan Larochelle, Lei Liu, Rachel Gunraj and Eduardo Candelario-Jalil; Project administration, Eduardo Candelario-Jalil; Resources, Eduardo Candelario-Jalil; Software, Changjun Yang and Eduardo Candelario-Jalil; Supervision, Antonio De Oliveira and Eduardo Candelario-Jalil; Validation, Changjun Yang and Eduardo Candelario-Jalil; Visualization, Changjun Yang, Antonio De Oliveira and Eduardo

Candelario-Jalil; Writing – original draft, Changjun Yang and Eduardo Candelario-Jalil; Writing – review & editing, Changjun Yang, Maria Machado da Silva, John Howell, Jonathan Larochelle, Lei Liu, Rachel Gunraj, Antonio De Oliveira and Eduardo Candelario-Jalil.

Funding

This work was supported by a Transformational Project Award from the American Heart Association (AHA; grant number 971058), and a grant R01NS129136 from the NINDS/NIH to ECJ,

Acknowledgment

We are grateful to Dr. John D. Harling for providing the RIPK2 PROTAC for our studies and facilitating the material transfer agreement between our laboratory and GlaxoSmithKline. MCMS thanks the CNPq (Fellowship number 200191/2021-7) for the Exchange Fellowship support. ACPdO acknowledges Coordenação de Aperfeiçoamento de Pessoal de Nível Superior - Brasil (CAPES; Finance Code 001; process #88887.682343/2022-00) for the Visiting Professor Fellowship.

References

1. Wicherska-Pawlowska, K.; Wrobel, T.; Rybka, J., Toll-Like Receptors (TLRs), NOD-Like Receptors (NLRs), and RIG-I-Like Receptors (RLRs) in Innate Immunity. TLRs, NLRs, and RLRs Ligands as Immunotherapeutic Agents for Hematopoietic Diseases. *Int J Mol Sci* **2021,** 22, (24).
2. West, A. P.; Koblansky, A. A.; Ghosh, S., Recognition and signaling by toll-like receptors. *Annu Rev Cell Dev Biol* **2006,** 22, 409-37.
3. Girardin, S. E.; Boneca, I. G.; Carneiro, L. A.; Antignac, A.; Jehanno, M.; Viala, J.; Tedin, K.; Taha, M. K.; Labigne, A.; Zahringer, U.; Coyle, A. J.; DiStefano, P. S.; Bertin, J.; Sansonetti, P. J.; Philpott, D. J., Nod1 detects a unique muropeptide from gram-negative bacterial peptidoglycan. *Science* **2003,** 300, (5625), 1584-7.
4. Girardin, S. E.; Boneca, I. G.; Viala, J.; Chamaillard, M.; Labigne, A.; Thomas, G.; Philpott, D. J.; Sansonetti, P. J., Nod2 is a general sensor of peptidoglycan through muramyl dipeptide (MDP) detection. *J Biol Chem* **2003,** 278, (11), 8869-72.
5. Kobayashi, K.; Inohara, N.; Hernandez, L. D.; Galan, J. E.; Nunez, G.; Janeway, C. A.; Medzhitov, R.; Flavell, R. A., RICK/Rip2/CARDIAK mediates signalling for receptors of the innate and adaptive immune systems. *Nature* **2002,** 416, (6877), 194-9.
6. Park, J. H.; Kim, Y. G.; McDonald, C.; Kanneganti, T. D.; Hasegawa, M.; Body-Malapel, M.; Inohara, N.; Nunez, G., RICK/RIP2 mediates innate immune responses induced through Nod1 and Nod2 but not TLRs. *J Immunol* **2007,** 178, (4), 2380-6.
7. Stanley, D.; Mason, L. J.; Mackin, K. E.; Srikhanta, Y. N.; Lyras, D.; Prakash, M. D.; Nurgali, K.; Venegas, A.; Hill, M. D.; Moore, R. J.; Wong, C. H., Translocation and

dissemination of commensal bacteria in post-stroke infection. *Nat Med* **2016,** 22, (11), 1277-1284.

8. Singh, V.; Roth, S.; Llovera, G.; Sadler, R.; Garzetti, D.; Stecher, B.; Dichgans, M.; Liesz, A., Microbiota Dysbiosis Controls the Neuroinflammatory Response after Stroke. *J Neurosci* **2016,** 36, (28), 7428-40.
9. Crapser, J.; Ritzel, R.; Verma, R.; Venna, V. R.; Liu, F.; Chauhan, A.; Koellhoffer, E.; Patel, A.; Ricker, A.; Maas, K.; Graf, J.; McCullough, L. D., Ischemic stroke induces gut permeability and enhances bacterial translocation leading to sepsis in aged mice. *Aging (Albany NY)* **2016,** 8, (5), 1049-63.
10. Ahnstedt, H.; Patrizz, A.; Chauhan, A.; Roy-O'Reilly, M.; Furr, J. W.; Spychala, M. S.; D'Aigle, J.; Blixt, F. W.; Zhu, L.; Bravo Alegria, J.; McCullough, L. D., Sex differences in T cell immune responses, gut permeability and outcome after ischemic stroke in aged mice. *Brain Behav Immun* **2020,** 87, 556-567.
11. Wu, X.; Lin, L.; Qin, J. J.; Wang, L.; Wang, H.; Zou, Y.; Zhu, X.; Hong, Y.; Zhang, Y.; Liu, Y.; Xin, C.; Xu, S.; Ye, S.; Zhang, J.; Xiong, Z.; Zhu, L.; Li, H.; Chen, J.; She, Z. G., CARD3 Promotes Cerebral Ischemia-Reperfusion Injury Via Activation of TAK1. *J Am Heart Assoc* **2020,** 9, (9), e014920.
12. Larochelle, J.; Tishko, R. J.; Yang, C.; Ge, Y.; Phan, L. T.; Gunraj, R. E.; Stansbury, S. M.; Liu, L.; Mohamadzadeh, M.; Khoshbouei, H.; Candelario-Jalil, E., Receptor-interacting protein kinase 2 (RIPK2) profoundly contributes to post-stroke neuroinflammation and behavioral deficits with microglia as unique perpetrators. *J Neuroinflammation* **2023,** 20, (1), 221.

13. Wang, M.; Ye, X.; Hu, J.; Zhao, Q.; Lv, B.; Ma, W.; Wang, W.; Yin, H.; Hao, Q.; Zhou, C.; Zhang, T.; Wu, W.; Wang, Y.; Zhou, M.; Zhang, C. H.; Cui, G., NOD1/RIP2 signalling enhances the microglia-driven inflammatory response and undergoes crosstalk with inflammatory cytokines to exacerbate brain damage following intracerebral haemorrhage in mice. *J Neuroinflammation* **2020,** 17, (1), 364.

14. Larochelle, J.; Howell, J. A.; Yang, C.; Liu, L.; Gunraj, R. E.; Stansbury, S. M.; de Oliveira, A. C. P.; Baksh, S.; Candelario-Jalil, E., Pharmacological inhibition of receptor-interacting protein kinase 2 (RIPK2) elicits neuroprotective effects following experimental ischemic stroke. *Exp Neurol* **2024,** 377, 114812.

15. Hall, H. T.; Wilhelm, M. T.; Saibil, S. D.; Mak, T. W.; Flavell, R. A.; Ohashi, P. S., RIP2 contributes to Nod signaling but is not essential for T cell proliferation, T helper differentiation or TLR responses. *Eur J Immunol* **2008,** 38, (1), 64-72.

16. Lu, C.; Wang, A.; Dorsch, M.; Tian, J.; Nagashima, K.; Coyle, A. J.; Jaffee, B.; Ocain, T. D.; Xu, Y., Participation of Rip2 in lipopolysaccharide signaling is independent of its kinase activity. *J Biol Chem* **2005,** 280, (16), 16278-83.

17. Watanabe, T.; Minaga, K.; Kamata, K.; Sakurai, T.; Komeda, Y.; Nagai, T.; Kitani, A.; Tajima, M.; Fuss, I. J.; Kudo, M.; Strober, W., RICK/RIP2 is a NOD2-independent nodal point of gut inflammation. *Int Immunol* **2019,** 31, (10), 669-683.

18. Chin, A. I.; Dempsey, P. W.; Bruhn, K.; Miller, J. F.; Xu, Y.; Cheng, G., Involvement of receptor-interacting protein 2 in innate and adaptive immune responses. *Nature* **2002,** 416, (6877), 190-4.

19. Nagamoto-Combs, K.; Kulas, J.; Combs, C. K., A novel cell line from spontaneously immortalized murine microglia. *J Neurosci Methods* **2014,** 233, 187-98.

20. DeMars, K. M.; Yang, C.; Castro-Rivera, C. I.; Candelario-Jalil, E., Selective degradation of BET proteins with dBET1, a proteolysis-targeting chimera, potently reduces pro-inflammatory responses in lipopolysaccharide-activated microglia. *Biochem Biophys Res Commun* **2018,** 497, (1), 410-415.

21. Mares, A.; Miah, A. H.; Smith, I. E. D.; Rackham, M.; Thawani, A. R.; Cryan, J.; Haile, P. A.; Votta, B. J.; Beal, A. M.; Capriotti, C.; Reilly, M. A.; Fisher, D. T.; Zinn, N.; Bantscheff, M.; MacDonald, T. T.; Vossenkamper, A.; Dace, P.; Churcher, I.; Benowitz, A. B.; Watt, G.; Denyer, J.; Scott-Stevens, P.; Harling, J. D., Extended pharmacodynamic responses observed upon PROTAC-mediated degradation of RIPK2. *Commun Biol* **2020,** 3, (1), 140.

22. Penna, I.; Vella, S.; Gigoni, A.; Russo, C.; Cancedda, R.; Pagano, A., Selection of candidate housekeeping genes for normalization in human postmortem brain samples. *Int J Mol Sci* **2011,** 12, (9), 5461-70.

23. Renard, M.; Vanhauwaert, S.; Vanhomwegen, M.; Rihani, A.; Vandamme, N.; Goossens, S.; Berx, G.; Van Vlierberghe, P.; Haigh, J. J.; Decaesteker, B.; Van Laere, J.; Lambertz, I.; Speleman, F.; Vandesompele, J.; Willaert, A., Expressed repetitive elements are broadly applicable reference targets for normalization of reverse transcription-qPCR data in mice. *Sci Rep* **2018,** 8, (1), 7642.

24. Strober, W.; Murray, P. J.; Kitani, A.; Watanabe, T., Signalling pathways and molecular interactions of NOD1 and NOD2. *Nat Rev Immunol* **2006,** 6, (1), 9-20.

25. Lee, K. H.; Biswas, A.; Liu, Y. J.; Kobayashi, K. S., Proteasomal degradation of Nod2 protein mediates tolerance to bacterial cell wall components. *J Biol Chem* **2012,** 287, (47), 39800-11.

26. Usluoglu, N.; Pavlovic, J.; Moelling, K.; Radziwill, G., RIP2 mediates LPS-induced p38 and IkappaBalpha signaling including IL-12 p40 expression in human monocyte-derived dendritic cells. *Eur J Immunol* **2007,** 37, (8), 2317-25.

27. Inohara, N.; Ogura, Y.; Fontalba, A.; Gutierrez, O.; Pons, F.; Crespo, J.; Fukase, K.; Inamura, S.; Kusumoto, S.; Hashimoto, M.; Foster, S. J.; Moran, A. P.; Fernandez-Luna, J. L.; Nunez, G., Host recognition of bacterial muramyl dipeptide mediated through NOD2. Implications for Crohn's disease. *J Biol Chem* **2003,** 278, (8), 5509-12.

28. Inohara, N.; Ogura, Y.; Chen, F. F.; Muto, A.; Nunez, G., Human Nod1 confers responsiveness to bacterial lipopolysaccharides. *J Biol Chem* **2001,** 276, (4), 2551-4.

29. Chamaillard, M.; Hashimoto, M.; Horie, Y.; Masumoto, J.; Qiu, S.; Saab, L.; Ogura, Y.; Kawasaki, A.; Fukase, K.; Kusumoto, S.; Valvano, M. A.; Foster, S. J.; Mak, T. W.; Nunez, G.; Inohara, N., An essential role for NOD1 in host recognition of bacterial peptidoglycan containing diaminopimelic acid. *Nat Immunol* **2003,** 4, (7), 702-7.

Figure legends

Figure 1. Dose- and time-dependent degradation of RIPK2 by its proteolysis targeting chimera in SIM-A9 cells. Model of RIPK2 degradation mediated by its proteolysis targeting chimera (PROTAC) molecule GSK3728857A (**A**) and the molecular structure of the RIPK2 PROTAC (**B**). Representative immunoblots and graphs showing degradation of RIPK2 by RIPK2 PROTAC in microglial cells. **C**, **D**) Incubation with various concentrations of RIPK2 PROTAC (0-10 μM) for 4 hours degrades RIPK2 in a dose-dependent manner. **E**, **F**) Similarly, time-dependent degradation of RIPK2 by the RIPK2 PROTAC (1 μM) was also observed. One-way ANOVA with Bonferroni post-test, **P*<0.05 and ****P*<0.001 compared with control conditions. Data are normalized to β-actin and represented as mean ± SEM from three to four independent experiments.

Figure 2. MDP dose-dependently induces pro-inflammatory gene expression in SIM-A9 cells. Graphs show treatment with various concentrations (0 to 10000 ng/mL) of muramyl dipeptide (MDP) for 24 hours dose-dependently increases transcription of pro-inflammatory genes *Nos2* (**A**), *Il-1β* (**B**), *Tnfα* (**C**), *Il6* (**D**) and *Mmp9* (**E**) in microglial cells. qRT-PCR data are normalized to the reference genes *Cyc1* and *Rltr2aiap* and represented as fold increases compared to control cells. One-way ANOVA with Bonferroni post-test, **P*<0.05, ***P*<0.01 and ****P*<0.001 compared with control conditions. Data are represented as mean ± SEM from four independent experiments.

Figure 3. RIPK2 PROTAC reduces MDP-induced pro-inflammatory gene expression and iNOS protein levels in SIM-A9 cells. SIM-A9 cells were pretreated with 1 μM RIPK2 PROTAC

for 4 h followed by 20 h incubation with 100 ng/mL MDP. After that, cells were harvested for RNA and protein extraction. **A**) Graph shows RIPK2 degradation by the RIPK2 PROTAC completely reduced MDP-induced transcription of pro-inflammatory genes *Nos2*, *Ptgs2*, *Il-1β*, *Tnfα*, *Il6*, *Ccl2,* and *Mmp9*. **B**-**E**) Effects of RIPK2 PROTAC on MDP-induced iNOS, COX-2, and RIPK2 protein levels. qRT-PCR data are normalized to the reference genes *Cyc1* and *Rltr2aiap* and represented as fold changes compared to MDP treatment, and immunoblot data are normalized to β-actin. One-way ANOVA with Bonferroni post-test, ***P<0.001. Data are represented as mean ± SEM from three independent experiments.

Figure 4. RIPK2 PROTAC suppresses activation of both NF-κB p65 and MAPK p38 induced by MDP in SIM-A9 cells. A) SIM-A9 cells were stimulated with 100 ng/mL MDP for the indicated periods (0 to 120 min). Immunoblots show MDP increased phosphorylation of NF-κB p65 and MAPK p38, and 60 min incubation of MDP induced the maximal effects on both phosphorylated protein levels. Data are representative of three independent experiments with similar results. **B**-**E**) SIM-A9 cells were pretreated with 1 μM RIPK2 PROTAC for 4 h followed by 60 min incubation of 100 ng/mL MDP. After that, cells were harvested for protein extraction and western blots. Immunoblots and graphs show that RIPK2 PROTAC completely abolished the effects of MDP on the phosphorylation of both NF-κB p65 (**B, C**) and MAPK p38 (**B, D**), which was associated with marked degradation of RIPK2 by its PROTAC pretreatment (**B, E**). One-way ANOVA with Bonferroni post-test, ***P<0.001. Data are normalized to β-actin and represented as mean ± SEM from three independent experiments.

Figure 5. Effects of RIPK2 PROTAC on LPS-induced pro-inflammatory gene expression, protein levels of iNOS and COX-2, and phosphorylated NF-κB p65 and MAPK p38 levels in SIM-A9 cells. SIM-A9 cells were pretreated with 1 μM RIPK2 PROTAC for 4 h followed by 20 h incubation with 10 ng/mL lipopolysaccharide (LPS). After that, cells were harvested for RNA and protein extraction. **A**) Graph shows that RIPK2 PROTAC partly reduced LPS-induced *Ptgs2*, *Il-1β*, *Il6*, *Ccl2* and *Mmp9* gene transcription, but did not affect the gene expression of *Nos2* and *Tnfα*. **B**-**E**) RIPK2 PROTAC had no effects on the LPS-induced increase in iNOS protein levels (**B, C**), but it slightly attenuated the LPS-induced upregulation of COX-2 levels (**B, D**). Treatment with RIPK2 PROTAC had no effects on increased levels of phosphorylated NF-κB p65 (**B, E**) or p38 MAPK (**B, F**) induced by LPS. At the same time, LPS-triggered upregulation of RIPK2 was potently degraded by its PROTAC (**B, G**). qRT-PCR data are normalized to the reference genes *Cyc1* and *Rltr2aiap* and represented as fold changes compared to LPS treatment, and immunoblot data are normalized to β-actin. One-way ANOVA with Bonferroni post-test, **P*<0.05, ***P*<0.01 and ****P*<0.001. Data are represented as mean ± SEM from three independent experiments.

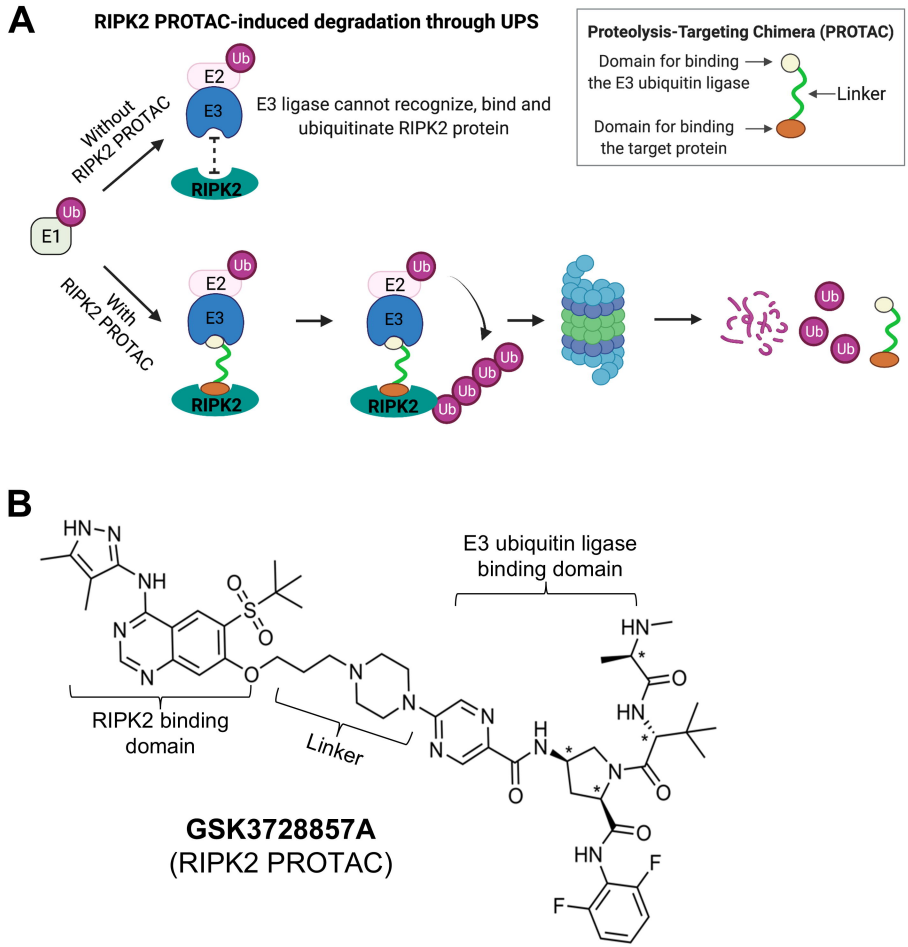
A
RIPK2 PROTAC-induced degradation through UPS
Proteolysis-Targeting Chimera (PROTAC)
Domain for binding the E3 ubiquitin ligase
Linker
Domain for binding the target protein
Without RIPK2 PROTAC
E3 ligase cannot recognize, bind and ubiquitinate RIPK2 protein
With RIPK2 PROTAC
Ub
E1
E2
E3
RIPK2
B
E3 ubiquitin ligase binding domain
RIPK2 binding domain
Linker
GSK3728857A
(RIPK2 PROTAC)
C
RIPK2 PROTAC (μM, 4 hours)
0 0.1 0.3 1 3 10
RIPK2
β-actin
62 kDa
42 kDa
D
RIPK2/β-actin
RIPK2 protac (μM)
E
RIPK2 PROTAC (1 μM, hours)
0 1 2 4 8 16 24
F
Time (hours)

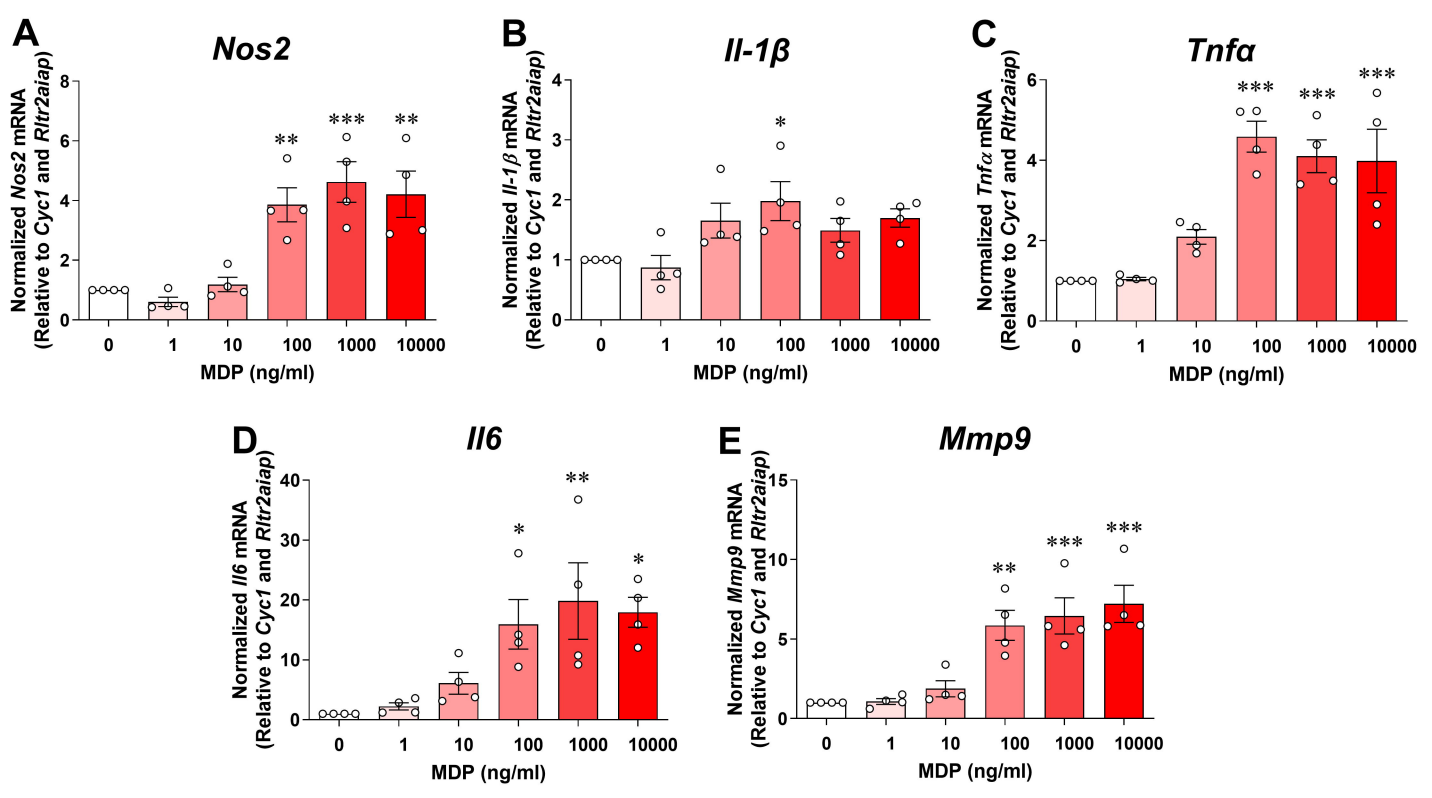
A
Nos2
Normalized Nos2 mRNA (Relative to Cyc1 and Rltr2aiap)
MDP (ng/ml)
B
Il-1β
Normalized Il-1β mRNA (Relative to Cyc1 and Rltr2aiap)
MDP (ng/ml)
C
Tnfα
Normalized Tnfα mRNA (Relative to Cyc1 and Rltr2aiap)
MDP (ng/ml)
D
Il6
Normalized Il6 mRNA (Relative to Cyc1 and Rltr2aiap)
MDP (ng/ml)
E
Mmp9
Normalized Mmp9 mRNA (Relative to Cyc1 and Rltr2aiap)
MDP (ng/ml)
0
1
10
100
1000
10000

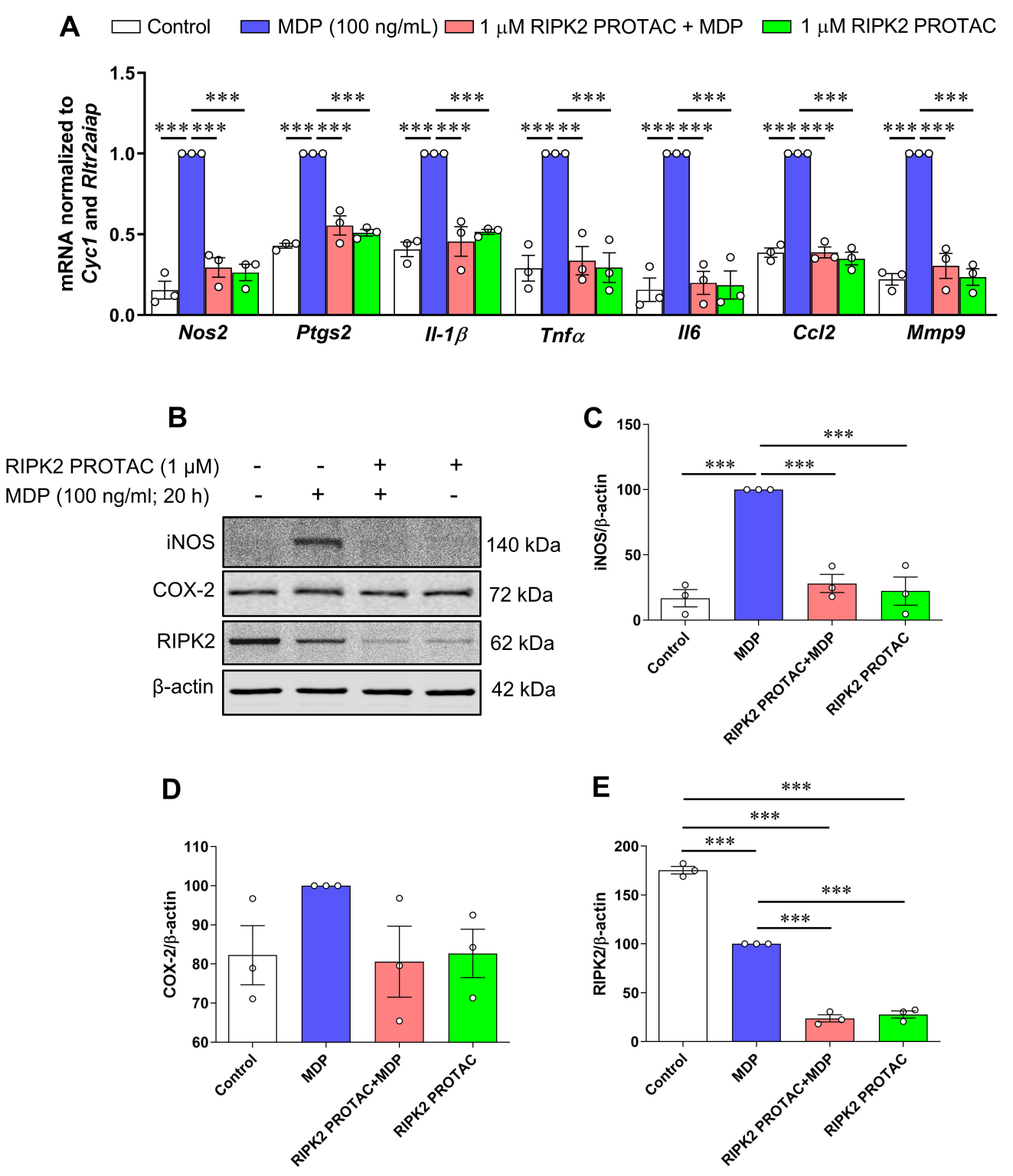
A
Control
MDP (100 ng/mL)
1 μM RIPK2 PROTAC + MDP
1 μM RIPK2 PROTAC
mRNA normalized to Cyc1 and Rltr2aiap
1.5
1.0
0.5
0.0
***
Nos2
Ptgs2
Il-1β
Tnfα
Il6
Ccl2
Mmp9
B
RIPK2 PROTAC (1 μM) - - + +
MDP (100 ng/ml; 20 h) - + + -
iNOS
COX-2
RIPK2
β-actin
140 kDa
72 kDa
62 kDa
42 kDa
C
iNOS/β-actin
150
100
50
0
Control
MDP
RIPK2 PROTAC+MDP
RIPK2 PROTAC
D
COX-2/β-actin
110
100
90
80
70
60
E
RIPK2/β-actin
200
150
100
50
0

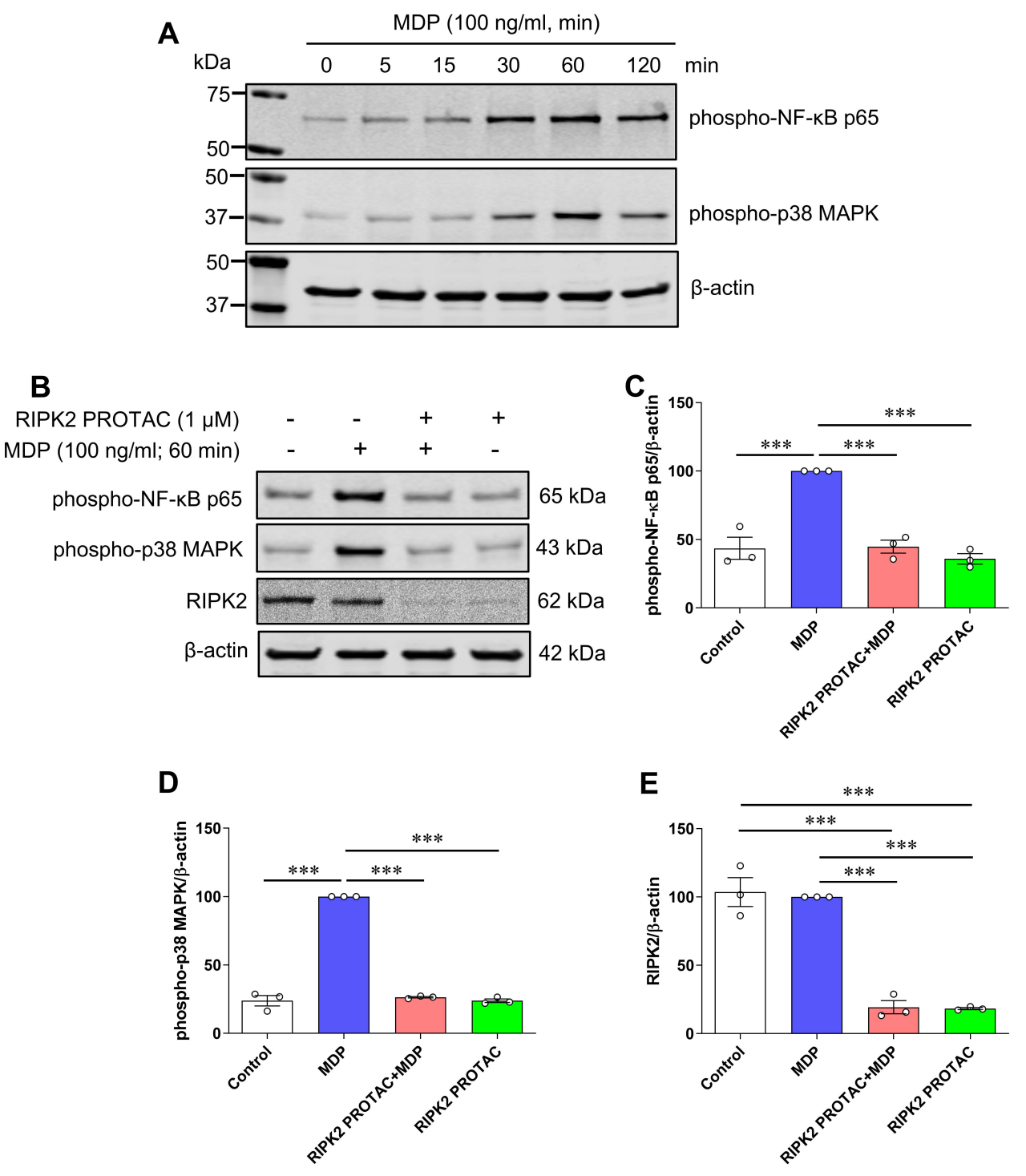
A
MDP (100 ng/ml, min)
kDa
0
5
15
30
60
120
min
75
50
50
37
50
37
phospho-NF-κB p65
phospho-p38 MAPK
β-actin
B
RIPK2 PROTAC (1 μM)
MDP (100 ng/ml; 60 min)
phospho-NF-κB p65
phospho-p38 MAPK
RIPK2
β-actin
65 kDa
43 kDa
62 kDa
42 kDa
C
phospho-NF-κB p65/β-actin
***
Control
MDP
RIPK2 PROTAC+MDP
RIPK2 PROTAC
D
phospho-p38 MAPK/β-actin
E
RIPK2/β-actin

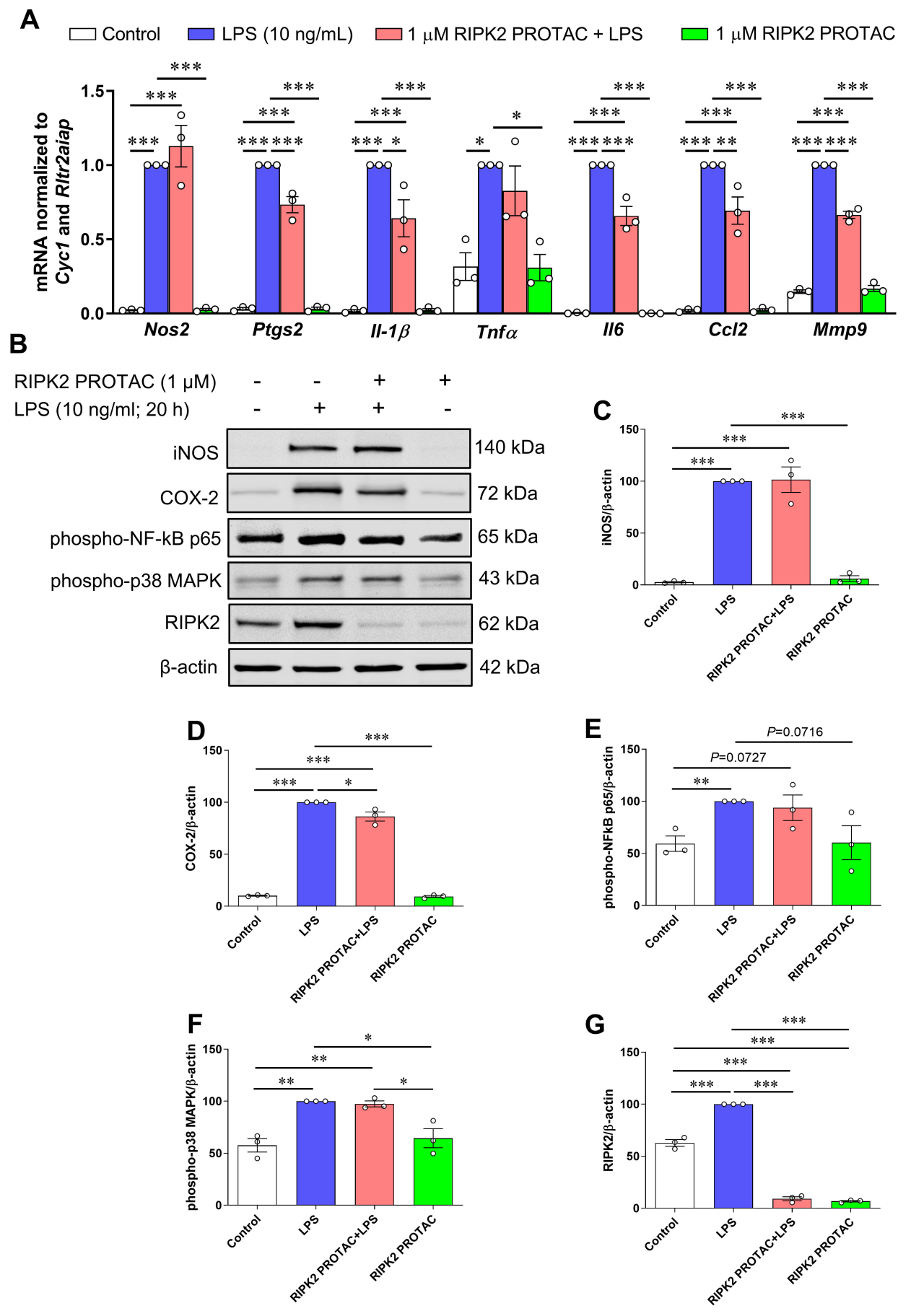
A
Control
LPS (10 ng/mL)
1 μM RIPK2 PROTAC + LPS
1 μM RIPK2 PROTAC
mRNA normalized to Cyc1 and Rltr2aiap
Nos2
Ptgs2
Il-1β
Tnfα
Il6
Ccl2
Mmp9
B
RIPK2 PROTAC (1 μM)
LPS (10 ng/ml; 20 h)
iNOS
COX-2
phospho-NF-kB p65
phospho-p38 MAPK
RIPK2
β-actin
140 kDa
72 kDa
65 kDa
43 kDa
62 kDa
42 kDa
C
iNOS/β-actin
D
COX-2/β-actin
E
phospho-NFkB p65/β-actin
P=0.0716
P=0.0727
F
phospho-p38 MAPK/β-actin
G
RIPK2/β-actin
Control
LPS
RIPK2 PROTAC+LPS
RIPK2 PROTAC